

See discussions, stats, and author profiles for this publication at: <https://www.researchgate.net/publication/230816627>

Photogeneration and Recombination in P₃HT/PCBM Solar Cells Probed by Time-Delayed Collection Field Experiments

ARTICLE *in* JOURNAL OF PHYSICAL CHEMISTRY LETTERS · APRIL 2011

Impact Factor: 7.46 · DOI: 10.1021/jz200155b

CITATIONS

88

READS

173

4 AUTHORS, INCLUDING:



Marcel Schubert

University of St Andrews

19 PUBLICATIONS 722 CITATIONS

SEE PROFILE



James C. Blakesley

National Physical Laboratory

27 PUBLICATIONS 1,212 CITATIONS

SEE PROFILE



Dieter Neher

Universität Potsdam

292 PUBLICATIONS 10,063 CITATIONS

SEE PROFILE

Photogeneration and Recombination in P3HT/PCBM Solar Cells Probed by Time-Delayed Collection Field Experiments

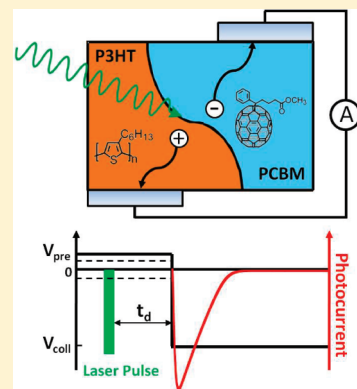
Juliane Kniepert, Marcel Schubert, James C. Blakesley, and Dieter Neher*

Institute of Physics and Astronomy, University of Potsdam, Karl-Liebknecht-Strasse 24-25, 14476 Potsdam, Germany

S Supporting Information

ABSTRACT: Time-delayed collection field (TDCF) experiments are performed on bulk heterojunction solar cells comprised of a blend of poly(3-hexylthiophene) and [6,6]-phenyl C₇₁ butyric acid methyl ester. TDCF is analogous to a pump–probe experiment using optical excitation and an electrical probe with a resolution of <100 ns. The number of free charge carriers extracted after a short delay is found to be independent of the electric field during illumination. Also, experiments performed with a variable delay between the optical excitation and the electrical probe do not reveal any evidence for the generation of charge via field-assisted dissociation of bound long-lived polaron pairs. Photocurrent transients are well fitted by computational drift diffusion simulations with only direct generation of free charge carriers. With increasing delay times between pump and probe, two loss mechanisms are identified; first, charge-carriers are swept out of the device by the internal electric field, and second, bimolecular recombination of the remaining carriers takes place with a reduced recombination coefficient.

SECTION: Macromolecules, Soft Matter



The primary photoexcitations in organic semiconductors are strongly bound Frenkel excitons. Consequently, efficient carrier generation in organic solar cells commonly relies upon the combination of an electron-donating (donor) and an electron-accepting (acceptor) component to separate the excitons into free charge carriers. For most of these devices, the photovoltaic properties are limited by processes at the donor–acceptor heterojunction.¹ Two conflicting models have been proposed to describe the elementary steps leading to the formation of extractable charge carriers.^{2,3} In the first model, the dissociation of excitons on either the donor or the acceptor component forms Coulombically bound electron–hole pairs (polaron pairs, PPs) at the heterojunction. While a small fraction of these PPs will always separate into free carriers by diffusion, the carrier generation yield is largely enhanced in the presence of an electric field. In the second model, exciton dissociation directly produces free carriers, meaning that the electric field should not affect the formation of extractable carriers.

To date, the combination of the donor polymer poly(3-hexylthiophene) (P3HT) with the soluble fullerene derivative [6,6]-phenyl C₇₁ butyric acid methyl ester (PCBM) is among the most efficient and well-studied systems.⁴ Bulk heterojunction layers are commonly formed by spincoating a 1:1 mixture of these two components from a suitable solvent. Slow drying, solvent soaking, or thermal annealing of the so-formed blend leads to a phase-separated morphology, comprised of an interpenetrating network of nanometer-sized crystalline domains. Solar cells comprised of these phase-separated blends exhibited external quantum efficiencies (EQE) in excess of 50%, open-circuit voltages (V_{oc}) close to 0.6 V, and fill factors (FF) above 60%. These high FFs imply that the photogenerated current depends only weakly on the internal field. This challenges the

view that the formation of free charges involves electric-field-assisted dissociation of Coulombically bound PPs. The analysis of the field-dependent photocurrents in P3HT/PCBM blends with the Onsager–Braun model requires PP lifetimes in excess of 1 μ s, which is well beyond the typical decay time of interfacial charge-transfer states in other systems.^{5–8} Recent Monte Carlo simulations, including hole delocalization on the P3HT chains, suggested that efficient PP dissociation might be achieved for an effective PP lifetime as short as 100 ns.⁹

As the decay of the interfacial PP to the ground state is mostly nonemissive in a blend of PCBM with regioregular P3HT,¹⁰ information on the kinetics of PP formation, dissociation, and recombination has been mainly gained from time-resolved transient absorption spectroscopy (TAS). R.H. Friend and co-workers applied bias-dependent TAS (at a fluence of 12 μ J/cm²) on as-prepared and annealed P3HT/PCBM (1:1) blends to differentiate between direct and field-assisted free charge generation.¹¹ Application of a reverse bias was shown to prolong the lifetime of the spectral feature attributed to holes on P3HT. This important observation was seen as direct proof for electric-field-assisted separation of interfacial PPs into free carriers. Other absorption, photoluminescence, and TAS studies on annealed P3HT/PCBM blends with different compositions also led to the conclusion that exciton dissociation and the survival of geminate recombination are the dominant factors determining solar cell performance.¹² On the other hand, intensity-dependent TAS studies on thermally annealed P3HT/PCBM blends by I.A.

Received: February 1, 2011

Accepted: February 25, 2011

Howard et al. and Ohkita et al. were consistently interpreted in terms of a rapid (within a few picoseconds) generation of free carriers, while loss due to monomolecular recombination of bound PPs was estimated to be 15% or less.^{13,14} Both studies were performed in the absence of an electric field, with fluences above $4 \mu\text{J}/\text{cm}^2$.

A general problem in TAS measurements is the simultaneous presence of different neutral and charged excitations, which often complicates the unequivocal distinction of bound charges (in PPs) and free (extractable) polarons. Furthermore, the change in absorbance due to excitons or polarons is small, and high fluences are normally required to obtain suitable signal-to-noise ratios. Here, we use bias-dependent time-delayed collection field (TDCF) experiments to probe the number of mobile (extractable) charge carriers in a phase-separated P3HT/PCBM blend with submicrosecond resolution and under small excitation densities. In a TDCF measurement, the sample is illuminated by a short laser pulse while being kept at constant prebias voltage V_{pre} .¹⁵ After the delay time t_d , a rectangular pulse with voltage V_{coll} is applied to extract all remaining free carriers. Therefore, TDCF is the analogue to TAS, with an electrical probe instead of an optical probe. In contrast to steady-state current–voltage measurements, classical time-of-flight experiments, or the photo-CELIV (charge extraction by a linearly increasing voltage) technique, TDCF allows one to apply different biases during generation and collection of the charge carriers. This enables a direct study on the field dependence of charge carrier generation and extraction. TDCF experiments on single-component organic layers revealed a pronounced dependence of the photogenerated mobile charge on the prebias during illumination.^{15–17} Later, the same method was used to study the recombination of photogenerated charges in a blend of PCBM with a soluble derivative of poly(*p*-phenylene vinylene).¹⁸ These experiments suggested that the photogenerated electrons and holes escaped the mutual Coulomb potential within the time resolution of the experiment (1 μs).

Samples for our study were prepared by coating a 1:1 blend of regioregular P3HT (Sepiolid P200, purchased from BASF) and PCBM (purchased from Solenne) from dichlorobenzene solution. Slow drying of the layer resulted in a phase-separated morphology, as revealed by the pronounced vibronic progression of the P3HT absorption in the spectrum of the blend.¹⁹ Indium tin oxide (ITO)-coated glass substrates covered with a ~ 60 nm thick layer of PEDOT/PSS (AI 4083 from H.C. Starck) served as the anode. The device was completed by thermal evaporation of 20 nm samarium capped with 100 nm aluminum. The active area of the device was 1 mm^2 , as defined by the geometric overlap of the ITO contact and the cathode (see Supporting Information for details about the sample design). The resulting sample capacitance was measured to be ~ 200 pF. With an active layer thickness of 200 nm, these devices exhibited a V_{oc} of ~ 0.55 V, a short-circuit current density J_{sc} of more than 10 mA/cm^2 , and FFs between 60 and 65% under AM 1.5 G illumination (see Figure S1 in the Supporting Information). The J_{sc} and the external quantum efficiency of these small-area devices were $\sim 20\%$ larger than those of the cells formed on the same substrate but with an active area of 16 mm^2 . We attribute this enhancement to edge effects and the absorption of stray light. Pulsed excitation (500 nm wavelength, 8 ns pulse width, 500 Hz repetition rate) from a diode-pumped, Q-switched Nd:YAG laser (NT242, EKSPLA) was used for TDCF measurements. The current through the device was measured via a 50 Ω resistor in series with the sample and was recorded with a YOKOGAWA DL9140

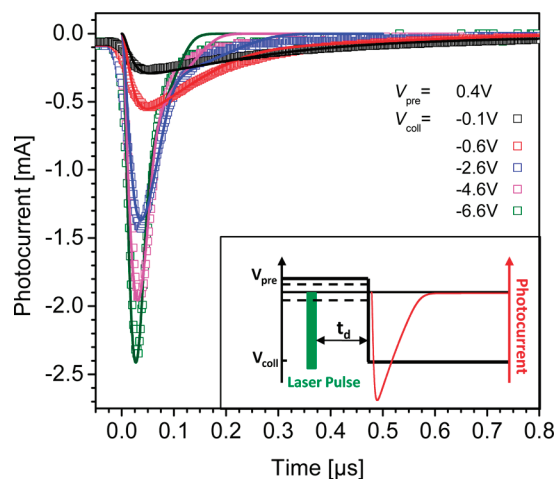


Figure 1. Experimental TDCF photocurrent transients (open squares) measured on a 200 nm thick layer of slow-dried P3HT/PCBM (1:1) with a prebias V_{pre} of 0.4 V and different values of the collection bias V_{coll} . The photocurrent transients were obtained from the difference between current transients with and without prior excitation of the sample. The collection bias was applied 150 ns after the laser pulse ($t = 0$ in this graph). Solid lines show fits to the data using a numerical drift diffusion model (for parameters see text). Inset: schematic timeline of the TDCF method indicating the experimental parameters V_{pre} , V_{coll} , and t_d .

digital oscilloscope. The overall RC time of the setup was 20 ns. The minimum delay between illumination and application of the collection field was 150 ns in our current setup.

Figure 1 shows TDCF photocurrent transients measured with a delay time t_d of 150 ns. The sample was kept at a prebias of 0.4 V (which is within the working regime of a solar cell) during excitation and prior to collection with V_{coll} . For low collection biases, the current transients are characterized by a steep increase (with the rise time determined by the sweep rate of the voltage generator, 15 ns, and the RC time constant of the detection system), followed by a gradual decay of the current. For weak collection fields, the decay is almost linear in time, which is consistent with the displacement of an initially homogeneous distribution of carriers with constant drift velocity. Under these conditions, an extrapolation of the linear part of the decay toward zero extraction current gives a rough estimate of the average carrier transit time. For higher reverse bias, the shape of the extraction transients becomes highly symmetric, with a half width of only 50 ns, which is determined by the instrumental time constants. Under these conditions, carriers are rapidly swept through the organic layer and extracted at the electrodes, meaning that the generation and recombination of carriers can now be studied with high time resolution. There is no indication in these photocurrent transients that the motion and extraction of electrons and holes occurs separately at well-distinguishable time scales. It has been shown that the mobility of electrons and holes is rather similar in slow-dried P3HT/PCBM layers.^{19,20} We found that all experimental transients in Figure 1 can be well described using a standard numerical drift diffusion model described in ref 21, with an electron mobility of $1.8 \times 10^{-7} \text{ m}^2 \text{ V}^{-1} \text{ s}^{-1}$, a hole mobility of $5 \times 10^{-8} \text{ m}^2 \text{ V}^{-1} \text{ s}^{-1}$, an initial (photogenerated) carrier density of $3.8 \times 10^{21} \text{ m}^{-3}$, a series resistance of 60 Ω , and the collection bias V_{coll} as the only variable parameter. Deviations between the numerical results and the experimental data are attributed to time- and field-dependent

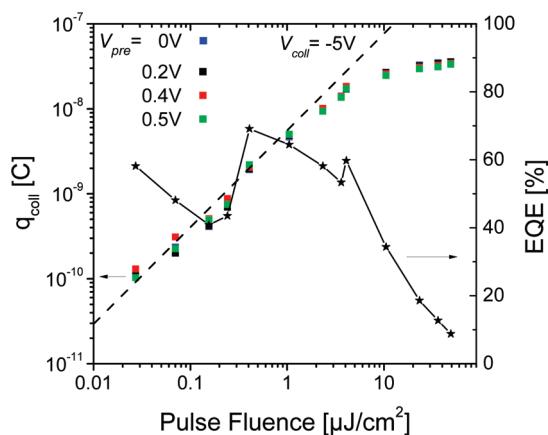


Figure 2. q_{coll} measured for different values of the prebias V_{pre} with a collection bias of $V_{\text{coll}} = -5$ V applied 150 ns after pulsed laser excitation. The dashed line indicates a linear dependence of the extracted charge on pulse fluence. The calculation of the external quantum efficiencies (EQE) as a function of pulse fluence was based on the average of the values of q_{coll} for different V_{pre} .

mobilities. Note that these simulations have been performed neglecting the bimolecular recombination, which will be addressed below in more detail.

We now turn to the integral of the photocurrent transient during collection, $q_{\text{coll}} = \int_{t_d}^{\infty} I_{\text{photo}}(t) dt$. If the displacement of the photogenerated charge prior to collection is insignificant, q_{coll} equals the initially photogenerated charge minus the charge lost due to recombination. This holds even in the case of strongly changing carrier mobilities (e.g., due to dispersion), nonuniform initial charge pair distributions, or when the external electric field is varied during extraction. q_{coll} is therefore a more reliable quantifier of photogenerated charge than can be provided by analysis of the magnitude or shape of I_{photo} (a more detailed discussion on the photocurrent integral can be found in the Supporting Information). Figure 2 plots the collected charge q_{coll} , calculated by integrating the experimental photocurrent transient during application of the collection bias and for a delay $t_d = 150$ ns. A high bias ($V_{\text{coll}} = -5$ V) was chosen to avoid recombination of photogenerated carriers during collection. Measurements were performed as a function of light intensity for different values of the prebias V_{pre} , representing typical operation conditions of a solar cell. q_{coll} follows a strictly linear increase with illumination intensity up to a pulse fluence of $\sim 1 \mu\text{J}/\text{cm}^2$, followed by a sublinear rise. This means that bimolecular recombination must be absent during collection at a bias of -5 V up to a photogenerated charge of $\sim 10^{-8}$ C (corresponding to an initial carrier density of $3 \times 10^{23} \text{ m}^{-3}$) and that all photogenerated free carriers (electrons and holes) are extracted under these conditions. In accordance with this conclusion, the values of the external quantum efficiency (EQE) calculated from the collected charge in the linear regime agree well with EQEs measured at short-circuit conditions and steady-state illumination. Note that Marsh et al. recently reported that the short-circuit photocurrent of a thermally annealed P3HT/PCBM blend measured under pulsed illumination increases linearly with intensity up to fluences of about $2\text{--}5 \mu\text{J}/\text{cm}^2$.¹¹ The significant decrease of the EQE under intense pulsed illumination was attributed to bimolecular nongeminate recombination processes, either charges or excitons. Howard et al. explained charge

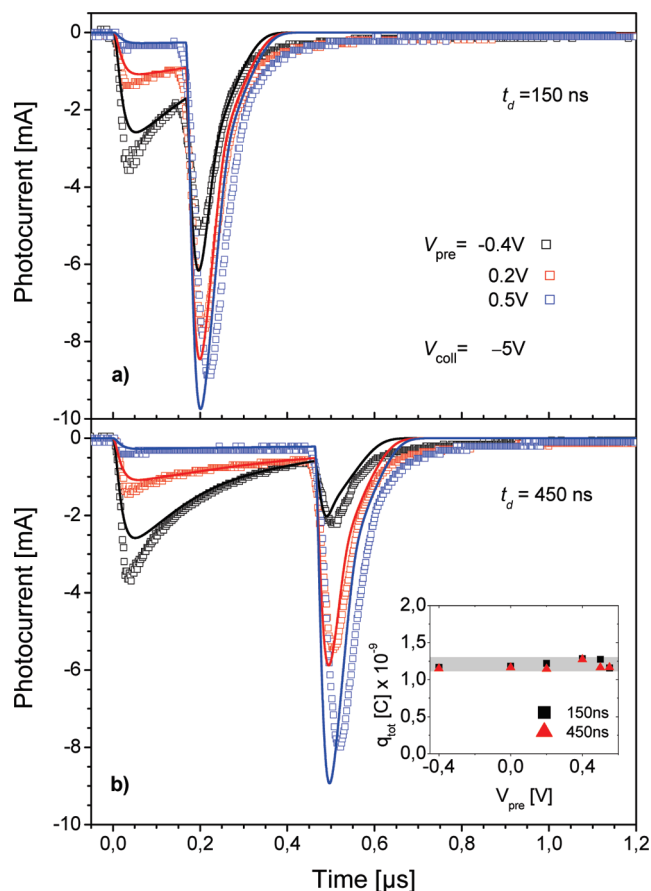


Figure 3. Experimental TDCF photocurrent transients (open squares) measured for a fixed collection bias V_{coll} of -5 V and different prebias V_{pre} for a time delay t_d between the laser pulse and a collection pulse of (a) 150 and (b) 450 ns. The sample was illuminated at $t = 0$ ns with a fluence of $0.4 \mu\text{J}/\text{cm}^2$. Also shown are the corresponding simulated transients (solid lines) with an electron mobility of $1.3 \times 10^{-7} \text{ m}^2 \text{ V}^{-1} \text{ s}^{-1}$, a hole mobility of $5 \times 10^{-8} \text{ m}^2 \text{ V}^{-1} \text{ s}^{-1}$, and an initial density of photogenerated carriers of $2.5 \times 10^{22} \text{ m}^{-3}$. The inset shows the integral over the entire photocurrent transient, q_{tot} , for different values of the prebias and delay times t_d of 150 (solid black squares) and 450 ns (solid red triangles). The shaded area indicates a 10% range around the mean value of 1.2×10^{-9} C.

population losses at fluences above $10 \mu\text{J}/\text{cm}^2$ observed in TAS on annealed P3HT/PCBM blends to be exciton charge annihilation at a time scale of a few picoseconds.¹³

Most noticeably, the charge available for extraction 150 ns after photoexcitation is virtually independent of the prebias. Though this observation is in favor of direct free carrier formation, we cannot rule out that exciton dissociation primarily produces long-lived PPs, which separate into free carriers under the high collection field. To test whether delayed separation of PPs contributes to the photocurrent, transients were recorded with different time delays t_d between the pulsed illumination and the application of the rectangular extraction voltage, with V_{pre} ranging between -0.4 and 0.55 V. We chose a fluence of $0.4 \mu\text{J}/\text{cm}^2$, which is ~ 1 order of magnitude below the onset of saturation in Figure 2. Under these conditions, the extracted charge is $\sim 1.2 \times 10^{-9}$ C, equivalent to a carrier density of $3.8 \times 10^{22} \text{ m}^{-3}$. It was recently shown that the carrier density in a thermally annealed P3HT/PCBM solar cell illuminated at 1 sun is between 5×10^{21}

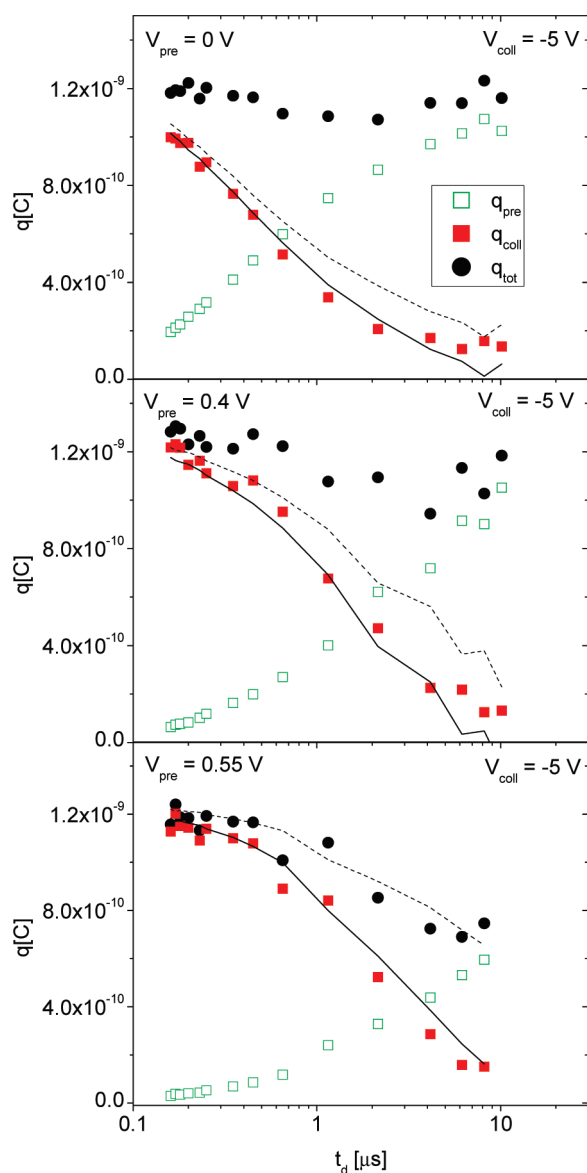


Figure 4. Integrated photocurrent under prebias, q_{pre} (open green squares), collection bias, q_{coll} (solid red squares), and $q_{\text{tot}} = q_{\text{pre}} + q_{\text{coll}}$ (solid black circles) as a function of delay time t_d for three different values of the prebias. The black solid lines have been calculated under the assumption of bimolecular recombination with a recombination coefficient of $5 \times 10^{-18} \text{ m}^3 \text{ s}^{-1}$ and an initial photogenerated charge of $1.20 \pm 0.05 \times 10^{-9} \text{ C}$ (eq 7 in the Supporting Information). The dashed lines show calculations with the same parameters but without loss due to bimolecular recombination.

and $1 \times 10^{23} \text{ m}^{-3}$ for an external bias between 0 and 0.6 V.²² Note that TAS experiments (with optical probe) use significant higher fluences.^{11,13}

Figure 3 shows exemplary transients measured for t_d of 150 and 450 ns. In all cases, a photocurrent is measured directly upon pulsed illumination, meaning that photoexcitation creates mobile charges on a time scale of less than 10 ns. With decreasing V_{pre} (increasing internal field during illumination), the photocurrent during prebiasing increases largely while the photocurrent peak during application of the collection field is reduced. These findings can be conclusively explained by assuming that the application of

a field during prebias extracts carriers from the active layer and reduces the amount of mobile carriers accessible for extraction at later times. On the other hand, these transients do not reveal any evidence for the delayed generation of charges via dissociation of a long-lived bound PP. Notably, we were able to reproduce the measured photocurrents in Figure 3 by drift diffusion simulations, assuming that photoexcitation generates the same initial density of photogenerated mobile carriers for all values of V_{pre} . Note that the simulated transients in Figure 3 use a constant electron and hole mobility (independent of carrier density and field). Therefore, the initial photocurrent spike upon illumination, attributed to the motion of hot carriers, and the tail of the photocurrent during collection due to the motion of relaxed carriers and detrapping are not well reproduced by these simulations.

Further information regarding the fate of the carriers in the blend after photoexcitation can be drawn by considering the integral of the photocurrent during prebias, $q_{\text{pre}}(t_d)$, and during collection, $q_{\text{coll}}(t_d)$, together with $q_{\text{tot}}(t_d) = q_{\text{pre}}(t_d) + q_{\text{coll}}(t_d)$ for different values of V_{pre} and t_d . For any delay, q_{tot} is equivalent to the total photogenerated charge that is extracted by the electrodes. The inset of Figure 3 plots q_{tot} for different prebiases and for delay times of 150 and of 450 ns. Within a tolerance range of 10%, the total extracted charge does not vary with the prebias. Therefore, field-assisted generation of carriers in competition with monomolecular recombination of geminate pairs must be insignificant within the first few hundreds of nanoseconds after photoexcitation, and the value $q_{\text{tot}} = 1.20 \pm 0.05 \times 10^{-9} \text{ C}$ for short delay is equal to the initial photogenerated charge $Q_{\text{photo}}^{\text{ini}}$ at a fluence of $0.4 \mu\text{J}/\text{cm}^2$.

Values of $q_{\text{pre}}(t_d)$, $q_{\text{coll}}(t_d)$, and $q_{\text{tot}}(t_d)$ for a wider range of t_d are plotted in Figure 4 (see Figure S2, Supporting Information, for additional data recorded with $V_{\text{pre}} = -0.4, 0.2, \text{ and } 0.5 \text{ V}$). Notably, the charge available for displacement and collection at longer delay times, $q_{\text{coll}}(t_d)$, decreases when the prebias becomes more negative, and this decrease becomes more significant with increasing t_d . Evidently, increasing the internal field during illumination (and prior to collection) does not increase the number of charge carriers available for displacement and collection after t_d . This finding is in apparent contradiction to the TAS studies by Marsh et al.¹¹ There, the prolonged lifetime of the hole-related spectral feature upon increasing electric field was interpreted as evidence that field-induced PP dissociation suppresses geminate recombination. Rather, we find that a more negative prebias accelerates the sweep-out of carriers during delay, leaving fewer to be extracted at later times. The TAS data of Marsh et al. can alternatively be explained by the mismatch in electron and hole mobilities. Rapid extraction of electrons under a negative bias leads to reduced bimolecular recombination in the remaining hole population. Therefore, the hole lifetime is increased, especially under the high fluences used in the TAS study.

As was stated above, $q_{\text{tot}}(t_d)$ measures the total photogenerated charge that survives recombination and is collected by the electrodes. V_{coll} is chosen to be sufficiently high to avoid recombination during collection, meaning that the difference between $Q_{\text{photo}}^{\text{ini}}$ and $q_{\text{tot}}(t_d)$ equals the total recombination loss during the delay time. For negative prebias, q_{tot} is virtually independent of delay time (see Figure S2, Supporting Information), meaning that recombination losses during delay are negligible under these conditions. This is due to rapid extraction of carriers under reverse prebias. However, as V_{pre} is increased to nearly open-circuit conditions, charge carriers remain in

the device long enough to undergo bimolecular recombination. This can be seen in the reduction in q_{tot} with increasing delay time. At the same time, the charge available for extraction after delay, $q_{\text{coll}}(t_d)$, becomes smaller than $Q_{\text{photo}}^{\text{ini}} - q_{\text{pre}}(t_d)$ (which describes the situation when neglecting recombination, see dashed lines in Figures 4 and S2, Supporting Information). To quantify the kinetics of recombination during delay, we have predicted $q_{\text{coll}}(t_d)$ by iterating forward in time from $t = 0$ under the presumption that all charges are subject to bimolecular recombination during delay and that V_{coll} collects all charges that remain in the layer after t_d (the solid curves in Figure 4). Here, the experimental $q_{\text{pre}}(t_d)$ values are used to quantify the displacement and extraction of charge during prebias. All data sets can be well described with an initial photogenerated charge of $1.20 \pm 0.05 \times 10^{-9}$ C and a bimolecular recombination coefficient of $\gamma = 5.0 \pm 0.5 \times 10^{-18} \text{ m}^3 \text{ s}^{-1}$. The value of γ is quite comparable to the coefficient for the recombination of freely mobile delocalized polarons determined recently by TAS in thermally annealed blends.¹⁴ On the other hand, γ is about 2 orders of magnitude smaller than the Langevin recombination coefficient $\gamma_1 = e(\mu_e + \mu_h)/\epsilon_0 \epsilon_r = 8.3 \times 10^{-16} \text{ m}^3 \text{ s}^{-1}$ predicted for three-dimensional recombination with the parameters given above. The comparison of the full and dashed lines in Figures 4 and S2 (Supporting Information) predicting $q_{\text{coll}}(t_d)$ with and without bimolecular recombination losses, respectively shows that the charge carrier dynamics can be fully explained by the competition between extraction and bimolecular recombination. Bimolecular recombination becomes increasingly important when V_{pre} approaches flat-band conditions; while nearly all photogenerated charge can be extracted at negative prebias. Bimolecular recombination reduces the extractable charge by nearly 50% for $V_{\text{pre}} = 0.55$ V.

In conclusion, we have used a bias-dependent time-delayed collection field to study the generation and recombination of charge carriers in slow-dried blends of P3HT with PCBM. For short delay times (up to ~ 500 ns), the photogenerated charge extracted by the electrodes is virtually independent of the prebias during illumination. We can, therefore, rule out that a significant number of mobile charge carriers are generated via the field-assisted dissociation of bound PPs in competition with geminate recombination within the first few hundred nanoseconds after photoexcitation. Also, the charge available for collection at longer delay times decreases when the prebias becomes more negative, meaning that the generation of free carriers via the dissociation of long-lived PPs is insignificant in these blends. Instead, the charge carrier kinetics can be quantitatively described by considering only the sweep-out of carriers out of the device by the internal electric field and losses due to bimolecular recombination of the remaining charge. Our conclusion complements well interpretations from very recent studies of P3HT/PCBM blends with transient absorption spectroscopy,^{13,14} which indicated direct generation of free charges within a few picoseconds. Our data also support the conclusion drawn from several other studies that current–voltage characteristics of a thermally annealed P3HT/PCBM blend cell depend on the competition between charge extraction and bimolecular recombination, without influence from geminate recombination.^{22–24}

■ ASSOCIATED CONTENT

S Supporting Information. Device layout, current–voltage characteristics of the solar cells, discussion of the photocurrent

integral, the integrated photocurrent q_{pre} , q_{coll} , and q_{tot} as a function of delay time recorded at $V_{\text{pre}} = -0.4, 0.2$, and 0.5 V, and description of the iterative simulation process to calculate the collected charge after delay t_d . This material is available free of charge via the Internet at <http://pubs.acs.org>.

■ AUTHOR INFORMATION

Corresponding Author

*Phone: +49 331 9771265. Fax: +49 331 977 5615. E-mail: neher@uni-potsdam.de.

■ ACKNOWLEDGMENT

The authors thank Jona Kurpiers and Andreas Pucher for laboratory assistance and Sarah Turner for her help editing the manuscript. This work was financially supported by the German Federal Ministry of Science and Education (BMBF) within SOHyb (FKZ 03X3525D) and the German Research Foundation (DFG) within the Priority Programme SPP 1355.

■ REFERENCES

- (1) Blom, P. W. M.; Mihailetschi, V. D.; Koster, L. J. A.; Markov, D. E. Device Physics of Polymer: Fullerene Bulk Heterojunction Solar Cells. *Adv. Mater.* **2007**, *19*, 1551–1566.
- (2) Deibel, C.; Strobel, T.; Dyakonov, V. Role of the Charge Transfer State in Organic Donor–Acceptor Solar Cells. *Adv. Mater.* **2010**, *22*, 4097–4111.
- (3) Clarke, T. M.; Durrant, J. R. Charge Photogeneration in Organic Solar Cells. *Chem. Rev.* **2010**, *110*, 6736–6767.
- (4) Brabec, C. J.; Gowrisanker, S.; Halls, J. J. M.; Laird, D.; Jia, S. J.; Williams, S. P. Polymer–Fullerene Bulk–Heterojunction Solar Cells. *Adv. Mater.* **2010**, *22*, 3839–3856.
- (5) Mihailetschi, V. D.; Xie, H. X.; de Boer, B.; Koster, L. J. A.; Blom, P. W. M. Charge Transport and Photocurrent Generation in Poly(3-hexylthiophene): Methanofullerene Bulk–Heterojunction Solar Cells. *Adv. Funct. Mater.* **2006**, *16*, 699–708.
- (6) Limpinsel, M.; Wagenpfahl, A.; Mingebach, M.; Deibel, C.; Dyakonov, V. Photocurrent in Bulk Heterojunction Solar Cells. *Phys. Rev. B* **2010**, *81*, 0852031–0852036.
- (7) Inal, S.; Schubert, M.; Sellinger, A.; Neher, D. The Relationship between the Electric Field-Induced Dissociation of Charge Transfer Excitons and the Photocurrent in Small Molecular/Polymeric Solar Cells. *J. Phys. Chem. Lett.* **2010**, *1*, 982–986.
- (8) Yin, C.; Schubert, M.; Bange, S.; Stiller, B.; Castellani, M.; Neher, D.; Kumke, M.; Hörhold, H. H. Tuning of the Excited-State Properties and Photovoltaic Performance in PPV-Based Polymer Blends. *J. Phys. Chem. C* **2008**, *112*, 14607–14617.
- (9) Deibel, C.; Strobel, T.; Dyakonov, V. Origin of the Efficient Polaron–Pair Dissociation in Polymer–Fullerene Blends. *Phys. Rev. Lett.* **2009**, *103*, 0364021–0364024.
- (10) Hallermann, M.; Kriegel, I.; Da Como, E.; Berger, J. M.; von Hauff, E.; Feldmann, J. Charge Transfer Excitons in Polymer/Fullerene Blends: The Role of Morphology and Polymer Chain Conformation. *Adv. Funct. Mater.* **2009**, *19*, 3662–3668.
- (11) Marsh, R. A.; Hodgkiss, J. M.; Friend, R. H. Direct Measurement of Electric Field-Assisted Charge Separation in Polymer: Fullerene Photovoltaic Diodes. *Adv. Mater.* **2010**, *22*, 3672–3676.
- (12) Keivanidis, P. E.; Clarke, T. M.; Lilliu, S.; Agostinelli, T.; Macdonald, J. E.; Durrant, J. R.; Bradley, D. D. C.; Nelson, J. Dependence of Charge Separation Efficiency on Film Microstructure in Poly(3-hexylthiophene-2,5-diyl):[6,6]-Phenyl-C₆₁ Butyric Acid Methyl Ester Blend Films. *J. Phys. Chem. Lett.* **2010**, *1*, 734–738.
- (13) Howard, I. A.; Mauer, R.; Meister, M.; Laquai, F. Effect of Morphology on Ultrafast Free Carrier Generation in Polythiophenes:

Fullerene Organic Solar Cells. *J. Am. Chem. Soc.* **2010**, *132*, 14866–14876.

(14) Guo, J. M.; Ohkita, H.; Benten, H.; Ito, S. Charge Generation and Recombination Dynamics in Poly(3-hexylthiophene)/Fullerene Blend Films with Different Regioregularities and Morphologies. *J. Am. Chem. Soc.* **2010**, *132*, 6154–6164.

(15) Popovic, Z. D. A Study of Carrier Generation Mechanism in X-Metal-Free Phthalocyanine. *J. Chem. Phys.* **1983**, *78*, 1552–1558.

(16) Esteghamatian, M.; Popovic, Z. D.; Xu, G. Carrier Generation Process in Poly(*p*-phenylene vinylene) by Fluorescent Quenching and Delayed-Collection-Field Techniques. *J. Phys. Chem.* **1996**, *100*, 13716–13719.

(17) Hertel, D.; Soh, E. V.; Bassler, H.; Rothberg, L. J. Electric Field Dependent Generation of Geminate Electron–Hole Pairs in a Ladder-Type π -Conjugated Polymer Probed by Fluorescence Quenching and Delayed Field Collection of Charge Carriers. *Chem. Phys. Lett.* **2002**, *361*, 99–105.

(18) Offermans, T.; Meskers, S. C. J.; Janssen, R. A. J. Time Delayed Collection Field Experiments on Polymer: Fullerene Bulk-Heterojunction Solar Cells. *J. Appl. Phys.* **2006**, *100*, 0745091–0745097.

(19) Li, G.; Shrotriya, V.; Huang, J.; Yao, Y.; Moriarty, T.; Emery, K.; Yang, Y. High-Efficiency Solution Processable Polymer Photovoltaic Cells by Self-Organization of Polymer Blends. *Nat. Mater.* **2005**, *4*, 864–868.

(20) Mihailetchi, V. D.; Xie, H. X.; de Boer, B.; Popescu, L. M.; Hummelen, J. C.; Blom, P. W. M.; Koster, L. J. A. Origin of the Enhanced Performance in Poly(3-hexylthiophene):[6,6]-Phenyl C₆₁-Butyric Acid Methyl Ester Solar Cells Upon Slow Drying of the Active Layer. *Appl. Phys. Lett.* **2006**, *89*, 0121071–0121073.

(21) Bange, S. Ph.D. Thesis, University of Potsdam, Germany, 2009.

(22) Shuttle, C. G.; Hamilton, R.; O'Regan, B. C.; Nelson, J.; Durrant, J. R. Charge-Density-Based Analysis of the Current–Voltage Response of Polythiophene/Fullerene Photovoltaic Devices. *Proc. Natl. Acad. Sci. U.S.A.* **2010**, *107*, 16448–16452.

(23) Street, R. A.; Cowan, S.; Heeger, A. J. Experimental Test for Geminate Recombination Applied to Organic Solar Cells. *Phys. Rev. B* **2010**, *82*, 121301.

(24) Mauer, R.; Howard, I. A.; Laquai, F. Effect of Nongeminate Recombination on Fill Factor in Polythiophene/Methanofullerene Organic Solar Cells. *J. Phys. Chem. Lett.* **2010**, *1*, 3500–3505.